Available online at www.sciencedirect.com
ScienceDirect
Journal of Power Sources 162 (2006) 1297–1303
JOURNAL OF POWER SOURCES
www.elsevier.com/locate/jpowsour

Influence of glyme-based nonaqueous electrolyte solutions on electrochemical properties of Si-based anodes for rechargeable lithium cells

Takashi Inose, Daisuke Watanabe, Hideyuki Morimoto, Shin-Ichi Tobishima *

Department of Chemistry, Faculty of Engineering, Gunma University, 1-5-1 Tenjincho, Kiryu, Gunma 376-8515, Japan

Received 21 June 2006; received in revised form 1 August 2006; accepted 1 August 2006
Available online 12 September 2006

Abstract

Influence of electrolyte solutions on charge–discharge properties of Si-based anodes were examined. As Si-based anodes, electrodes prepared from (i) a mixture of Si and carbon (Si + C) and (ii) a mixture of a Si–SiO_2–C composite and carbon (Si–C + C) were used. As electrolyte solutions, ethylene carbonate (EC)/methylethyl carbonate (MEC)/*n*-glyme ternary mixed solvent with 1 M (M: mol L^{-1}) $LiPF_6$ was used. Poly(ethylene glycol) dimethyl ethers [$(CH_3O(CH_2CH_2O)_nCH_3$, $n = 1, 2, 3$ and 4)] are generally known as "glymes". In case of Li/Si + C cells, by mixing glymes to 1 M $LiPF_6$-EC/MEC (30:70 in mixing volume percentage; EM), discharge capacity tended to become larger than that with EM alone. Cycle life of Li/Si + C cells was approximately the same when different electrolyte solutions were used. Primary reason for the degradation of charge–discharge cycling life of Li/Si + C cells is a physical breakdown and loosing electronic conductive path of Si electrode. This phenomenon was resulted from a large volume change of electrode by expansion and shrinking of Si during charge–discharge of lithium in Si. Also, reactivity of electrolyte solutions toward lithium affected the degradation of charge–discharge capacity. Discharge capacity depended on a reduction potential (E_{red}) of glymes, not on an electrolyte conductivity (κ). In case of Li/Si–C + C cells, by mixing *n*-glymes to EM, the discharge capacity tended to become larger than that with EM alone. Cycling life of Li/Si–C + C cells improved, compared with that of Li/Si + C cells. This was due to a suppression of physical breakdown by Si–C structure with a thin carbon surface layer on it. Influence of reactivity of electrolyte solutions toward lithium on the degradation of charge–discharge capacity of Li/Si–C + C cells was much smaller than that of Li/Si + C cells. Discharge capacity of Li/Si–C + C cells depended on κ, not on Ered.

Keywords: Lithium cell; Electrolyte; Glyme; Si-electrode; Rechargeable cell

1. Introduction

Many of commercial lithium ion cells are composed of carbon anodes, $LiCoO_2$ cathodes and nonaqueous electrolyte solutions. Typical example of nonaqueous electrolyte solutions is LiPF6–ethylene carbonate (EC)/methylethyl carbonate (MEC). Enhancement of energy density of lithium ion cells has been required every year. However, now practical capacity of carbon anodes is getting closer to a theoretical value of graphite (372 mAh g^{-1}). Then, new anode materials having higher capacity density than those of carbon materials have been studied. Examples of these materials are various Si-based compounds including Si [1–15].

Si reacts with lithium and finally forms $Li_{22}Si_5$ ($Li_{4.4}Si$), which has a theoretical capacity density of 2400 mAh cm^{-3} and 4200 mAh g^{-1} [1,2]. These capacity densities are considerably larger than those of C_6Li (740 mAh cm^{-3} and 372 mAh g^{-1}). However, one of the problems of Si-based anodes is their poor cycleability. Degradation of cycling performance is caused by a physical break-down and loosing an electronic conductive path of electrode, resulted from a large volume change of Si anode during charge–discharge of lithium in Si. Si swells and becomes 3.8 times larger after $Li_{4.4}Si$ forms [1,2]. To suppress this phenomenon, many researches have been carried out. Examples of these researches are coating Si surface with carbon films [8–11], various Si alloys [1,3–7] and a Si–SiO_2–C composite

* Corresponding author. Tel.: +81 277 30 1382; fax: +81 277 30 1380.
E-mail address: tobi@chem.gunma-u.ac.jp (S.-I. Tobishima).

0378-7753/$ – see front matter © 2006 Elsevier B.V. All rights reserved.
doi:10.1016/j.jpowsour.2006.08.005

Table 1
Physical properties and abbreviations of the solvents

Solvent (abbreviations)	Fp (°C)	mp (°C)	bp (°C)	η_0 (cP) at 25 °C	ε at 25 °C	V_s (nm^3)	DN
Monoglyme (DME)	0	−69	85.2	0.46	5.5	0.170	24
Diglyme (DIG)	70	−64	162.0	0.98	5.8	0.236	19.2
Triglyme (TRG)	110	−45	216.0	3.80	7.5	0.300	14.0
Tetraglyme (TEG)	140	−27	275.3	4.05	7.9	0.364	16.6
Ethylene carbonate (EC)	160	36	248	2.53[a]	95 (89)[b]	0.118	16.4
Methylethyl carbonate (MEC)	23	−54	107	0.70	2.9	0.171	6.5

Fp: flash point; mp: melting point; bp: boiling point at 1 Torr; η_0: viscosity; ε: dielectric constant; V_s: molecular volume; DN: donor number.
[a] EC/PC (6:1).
[b] At 40 °C.

compounds [14–16]. Also, electrolyte solutions should affect the charge–discharge cycling performance of Si-based electrodes. However, there are many ambiguous factors about how electrolyte solutions affect the charge–discharge properties of Si-based electrodes.

Influence of electrolyte solutions on charge–discharge cycling efficiency of lithium metals and carbon anodes is generally discussed as follows [17].

In case of lithium metals, two important factors for degradation of cycling performance are discussed. First is lithium deposition morphology. When lithium is plated (charged), dendrite deposition of lithium tends to occur. Then, exfoliation of lithium from electrode occurs. Second, plated fresh lithium is chemically reactive. Then, plated lithium reacts with electrolyte solutions. This reaction is a reduction of electrolyte solutions by lithium. Products are generally solid and gas compounds. So, lithium is chemically consumed before discharge. Therefore, cycling efficiency of lithium metal anode is less than 100%.

In case of carbon anodes, at first charging (lithium insertion to carbon), C_6Li_x electrochemically reacts with electrolyte solutions. Chemical composition of products is reported to be the same as that in case of lithium metal [18]. However, in case of carbon, this solid products works as a protective surface film on anode, which is so called "SEI (solid electrolyte interface)" [17]. Lithium consumption for SEI formation leads an irreversible capacity between first charge and discharge of carbon anodes. Lithium ions can pass through SEI though solvents cannot. Physical properties of surface film are important. Whether products works as good SEI for realizing good cycleability or not depends on electrolyte solutions.

In case of Si-based anodes, similar reaction mentioned above may occur. However, it is not clear whether influence of electrolyte solutions is similar to lithium metals, or similar to intercalation compounds such as carbons, or completely different from these two anodes.

Other while, we have reported that LiPF6-EC/MEC/glyme ternary mixed solvent electrolytes exhibits both higher cycling efficiency of lithium metal anodes and higher conductivity than those of EC/MEC binary mixed solvent electrolyte [19]. Polyethylene glycol dialkyl ethers are generally known as "glymes", which have a general, chemical formula shown in Eq. (1). We have investigated the properties of polyethylene glycol dimethyl ethers [$R_1 = R_2 = CH_3$, $n = 1$, 2, 3 and 4 in Eq. (1)]. These symmetric glymes are called as monoglyme ($n = 1$), diglyme ($n = 2$, DIG), triglyme ($n = 3$, TRG) and tetraglyme ($n = 4$, TEG). Monoglyme is a famous solvent generally known as 1,2-dimethoxyethane (DME). Table 1 shows physical properties of glymes:

$$R_1O(CH_2CH_2O)_nR_2 \quad (1)$$

In this study, influence of glyme-based electrolytes on charge–discharge cycling properties of lithium in two types of Si-based anodes is preliminarily examined. As Si-based anodes: (i) anodes prepared from a mixture of Si and carbon (Si + C), and (ii) anodes prepared from a mixture of carbon and a Si–SiO_2–carbon composite (Si–C + C) are examined. As electrolyte solutions, 1 M LiPF6-EC/MEC/glyme ternary mixed solvent electrolytes are used.

2. Experimental

2.1. Electrolyte preparations

Electrolyte solutions were prepared as described previous paper [18]. The water content of the test solutions was less than 20 ppm, which was determined by Karl–Fisher titration method. Hereafter, "EM" will represent an electrolyte solution of 1 M $LiPF_6$-EC/MEC (30:70 in mixing volume percentage). As the glyme-based electrolytes, 1 M $LiPF_6$-$EM_{(100-x)}$/n-$glyme_{(x)}$ ternary mixed solvent electrolytes are used, where x means a mixing volume percentage of n-glyme in EM + n-glyme. $x = 60$ for monoglyme (DME), $x = 30$ for diglyme (DIG), $x = 20$ for

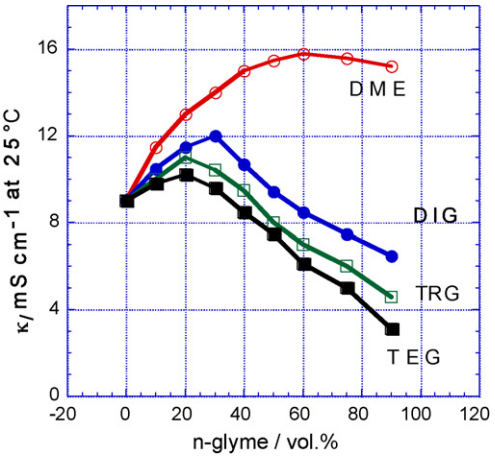

Fig. 1. Conductivity (κ) of 1 M $LiPF_6$-[EC/MEC(3:7)]/n-glyme at 25 °C.

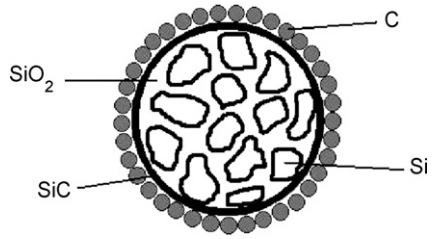

Fig. 2. Image of Si–SiO_2–carbon composite (Si–C).

triglyme (TRG) and tetraglyme (TEG) were used. Because these electrolyte composition exhibited the maximum conductivity (κ) at 25 °C (Fig. 1).

2.2. Si-based electrode materials

Two types of Si-based anodes were used. That is (i) anodes prepared from a mixture of Si and carbon (Si + C), and (ii) anodes prepared from a mixture of carbon and a Si–SiO_2–carbon composite (Si–C + C) are examined. The printed Si + C electrodes were prepared by coating a Cu sheet with a mixture of Si or Si–C, carbon (graphite) powder and poly (vinylidene fluoride) (PVDF) in *N*-methyl pyrolidinone (NMP) (the weight ratio of Si:carbon:binder = 46.4:41:4:12.5). Particle size of Si, graphite and Si–C was 5, 3 and 10 μm. We then evacuated the solvent and dried the electrodes. The printed carbon electrodes are 15 mm in diameter and 0.15 mm in thickness. Si–C (a Si–SiO_2–carbon composite) material was prepared according to the papers [14–16] by methane–argon gas mixture-chemical vapor deposition (CVD) with 1100 °C heat treatment for SiO. Schematic illustration of the final product of Si–C material is shown in Fig. 2. Fine silicon crystal was distributed in the SiO_2. The surface of the final product was covered with double layers composed of thin inside layer of SiC (silicon carbide) and thick outside layer of carbon. The printed Si–C + C electrodes were prepared by similar preparation method to that of Si + C electrodes as mentioned above.

2.3. Lithium cycling efficiency measurements

Charge–discharge cycling tests were carried out galvanostatically by the charge–discharge voltage cut-off (0 and 1.5 V versus Li/Li+) with a constant current density (I_{ps}) of 0.5 mA cm^{-2} by using coin cells (coin type 2032, diameter 20 mm in diameter, 3.2 mm in thickness). These cells have a lithium metal sheet counter electrode (0.1 mm thickness, 15 mm diameter) and the working printed electrode of Si–C or Si–C + C.

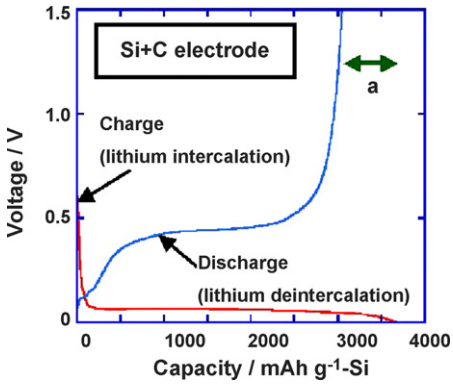

Fig. 4. Charge–discharge voltage profile of Li/Si + C cell at first cycle in EM, I_{ps} = 0.5 mA cm^{-2}, charge–discharge cut-off voltages: 0 and 1.5 V, a: irreversible capacity.

Fig. 3 shows XRD pattern of Si + C and Si–C + C electrodes. XRD of Si + C electrode shows sharp peaks of Si, C and Cu. Cu is a substrate of the printed electrode. XRD of Si–C + C electrode shows broad and weak peaks. This XRD pattern of Si–C + C may be caused by the existence of amorphous SiO_2 and/or the phenomenon that the electrode surface is covered with double layers composed of thin inside layer of SiC and thick outside layer of carbon.

All the electrochemical measurements were carried out at 25 °C.

3. Results and discussion

3.1. Charge–discharge cycling properties of lithium in Si-based electrodes with EM

Fig. 4 shows charge and discharge voltage curves of a Li/Si + C cell at first cycle with EM electrolyte. Here, charge and discharge mean lithium intercalation into Si (alloying) and deintercalation from it, respectively. Charge voltage curve exhibited plateau of approximately 0.1 mV. The first charge capacity

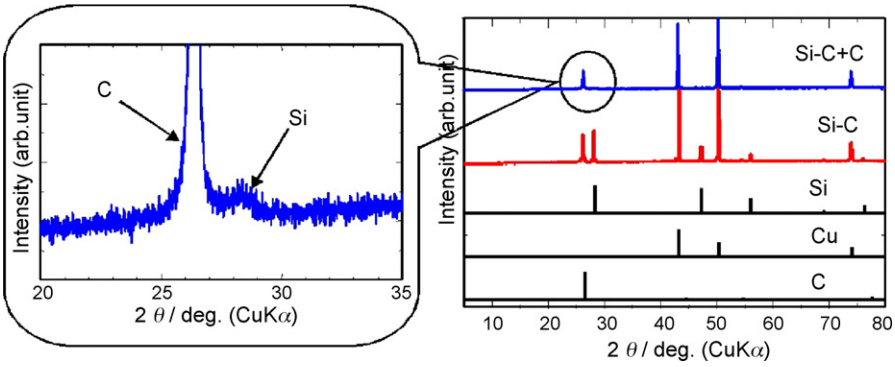

Fig. 3. XRD pattern of Si + C and Si–C + C electrodes.

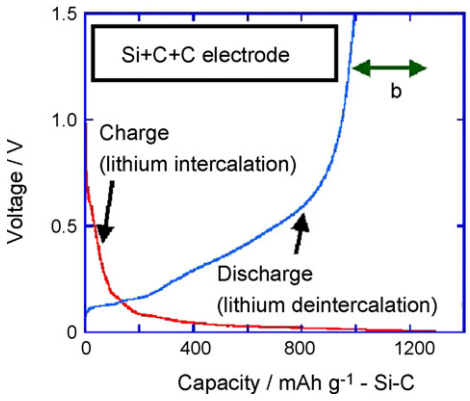

Fig. 5. Charge–discharge voltage profile of Li/Si–C + C cell at first cycle in EM, I_{ps} = 0.5 mA cm^{-2}, charge–discharge cut-off voltages: 0 and 1.5 V, b: irreversible capacity.

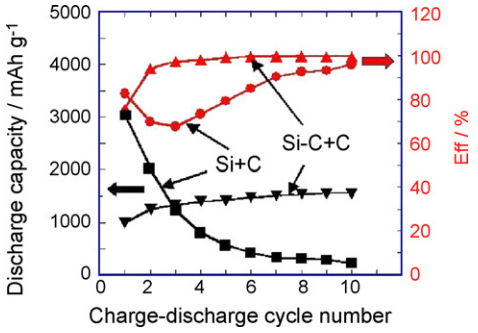

Fig. 6. Charge–discharge cycling tests results of Li/Si + C and Li/Si–C + C cells in EM, I_{ps} = 0.5 mA cm^{-2}, charge–discharge cut-off voltages: 0 and 1.5 V.

was 3700 mAh g^{-1} (per Si weight). This capacity corresponds to a formation of $Li_{3.88}Si$. When lithium is discharged from $Li_{3.88}Si$, voltage exhibited plateau of approximately 0.4 mV and increased after it. Discharge capacity was 3080 mAh g^{-1} (3.23Li discharge from $Li_{3.88}Si$). The irreversible capacity was 620 mAh g^{-1}. Charge–discharge cycling efficiency (=discharge capacity/charge capacity, E_{ff}) was 83.2%. This irreversible capacity results mainly from electrochemical reduction of electrolyte solution on the Si–C electrode surface. This irreversible capacity may also include a small capacity of lithium, which is trapped in Li_xSi lattice and cannot discharge.

Fig. 5 shows charge and discharge voltage curves of a Li/Si–C + C cell at first cycle with EM electrolyte. When the cell was charged (lithium was intercalated into Si), the charge voltage curve sloped gently. The first charge capacity was 1230 mAh g^{-1} (per Si–C weight). When lithium is extracted from Li_xSi–C, the discharge voltage sloped. These voltage slopes in a charge and discharge voltage profile may arise from an amorphous state of Si–C. The first discharge capacity was 1020 mAh g^{-1}. The irreversible capacity was 210 mAh g^{-1}. charge–discharge cycling efficiency (E_{ff}) was 82.9%. This efficiency of Si–C + C was approximately the same as that of Si + C. In case of Si–C + C electrodes, this irreversible capacity may contain a capacity of Li_2O formation [14–16].

Fig. 6 shows charge–discharge cycling test results of Li/Si + C and Li/Si–C + C cells with EM electrolyte. Li/Si + C cell exhibited higher discharge capacity than that of Li/Si–C + C cell at first and second cycle. However, the discharge capacity of Li/Si + C cell rapidly decreased with an increase in a cycle number. At third cycle, discharge capacity of Li/Si + C cell became smaller than that of Li/Si–C + C cell. Cycling efficiency (E_{ff}) of Li/Si + C cell was far from 100% from first to eighth cycle. That is, large irreversible capacities exist from first to eighth cycles for Li/Si + C cells. Other while, in case of Li/Si–C + C cell, the discharge capacity gradually increases with an increase in a cycle number from first to fourth cycle. The discharge capacity became a constant value of 1500 mAh g^{-1} after third cycle. Charge–discharge efficiency (E_{ff}) was constant of approximately 100% after third cycle. There was no irreversible capacity after third cycle for Li/Si–C + C cells. The cycling capacity of Li/Si–C cell was about 1/3 of the maximum capacity of Li/Si + C

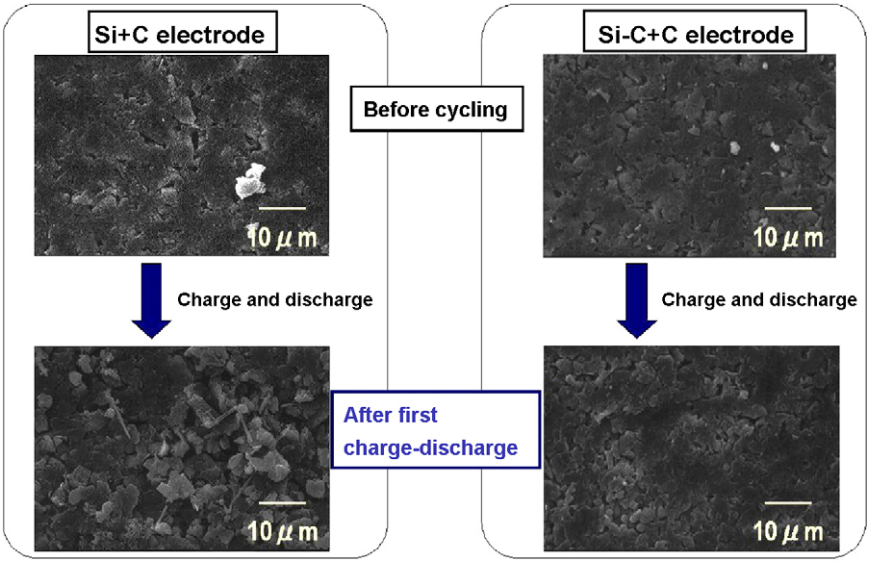

Fig. 7. SEM photographs of Si + C and Si–C + C electrode after first charge and discharge in EM, I_{ps} = 0.5 mA cm^{-2}, charge–discharge cut-off voltages: 0 and 1.5 V.

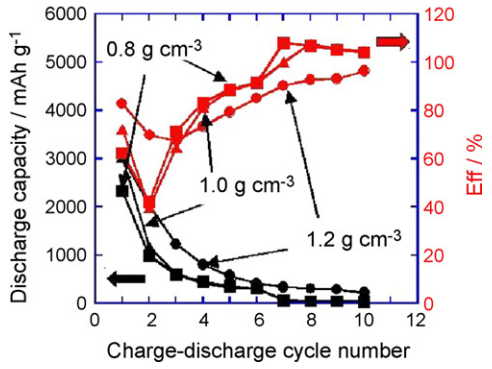

Fig. 8. Charge–discharge cycling tests results of Li/Si + C cells in EM, I_{ps} = 0.5 mA cm^{-2}, charge–discharge cut-off voltages: 0 and 1.5 V.

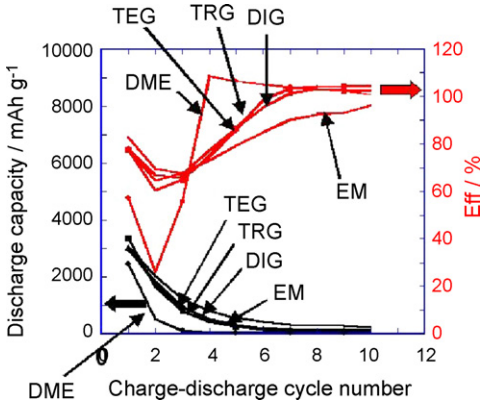

Fig. 9. Relationships among a discharge capacity, a charge–discharge cycling efficiency (E_{ff}) and a cycle number of Li/Si + C cells with EM/glyme electrolytes, I_{ps} = 0.5 mA cm^{-2}, charge–discharge cut-off voltages: 0 and 1.5 V.

cells. However, the cycling stability (cycling efficiency versus cycle number) of Li/Si–C + C cells is better than that of Li/Si + C cells.

Fig. 7 shows SEM photographs of Si + C and Si–C + C electrodes before and after first charge–discharge cycling. In case of Si + C electrode, the electrode surface became very rough after charge–discharge cycle. These phenomena result from a physical break down of electrode by large swelling and shrinking after charge–discharge of Li in Si. This is main reason for the bad cycling performance of Si + C electrodes. Also, this roughness of electrodes causes an increase in a reaction surface area of Li_xSi toward electrolyte solution. In case of Si–C + C electrode, the surface after charge–discharge was similar to that before charge–discharge. Then, Si–C structure with a thin outside layer of carbon suppresses the electrode breakdown and leads a better cycling performance than that of Si + C electrode.

Fig. 8 shows an influence of electrode density on charge–discharge cycling properties of Li/Si + C cells. With an increase in an electrode density, the discharge capacity tended to increase. This result is considered to result from the following reason. With a decrease in a density, the void in the electrode tends to increase. Then, an electronic conductive path tends to break with a large expansion and shirking during charge–discharge of lithium in Si. Then, Si + C electrodes of density of 1.2 g cm^{-3}, the largest density examined here, were used for the investigation of an influence of electrolyte solutions on charge–discharge cycling properties.

3.2. Charge–discharge cycling properties of lithium in Si + C electrodes with EM/n-glyme electrolyte solutions

Using a Li/Si + C coin cell with EM/*n*-glymes carried out charge–discharge cycling tests of lithium. Figs. 9 and 10 show the charge–discharge cycling test results. Fig. 9 shows the relationship among a discharge capacity, a charge–discharge cycling efficiency (E_{ff}) and a cycle number. Fig. 10 shows the relationship among a discharge capacity at first cycle, an electrolyte conductivity (κ) and a reduction potential (E_{red}) of *n*-glymes. Following five results were obtained from these two figures. (1) Discharge capacities depended on the kind of electrolyte solutions. (2) Discharge capacity at first cycle was high in the order of EM/TEG > EM/TRG > EM/DIG > EM > EM/DME. By mixing *n*-glymes to EM, the discharge capacity tended to become larger than that with EM alone, except for DME. (3) There was no distinct relationship between the discharge capacity and κ. (4) With an increase in an E_{red} (becoming noble), the discharge capacity tended to decrease. (5) Cycle life of all the cells was approximately 10 cycles.

Summarizing these results, primary cause for the cycle life degradation is suggested to be physical breakdown of Si + C electrode by the large expansion and shirking during charge and discharge of lithium in Si. Additional cause of cycle life degradation is the influence of electrolyte solutions. The model of the influence of the electrolyte solutions on the charge–discharge of lithium in Si + C was proposed (Fig. 11). Si + C were prepared by simply mixing Si and carbon. Then, there is both Si surface and carbon surface on the electrode surface. Lithium ions are solvated selectively with *n*-glyme molecules in EM/glyme electrolyte solutions [19]. During charging, at first step, lithium ions with solvent molecules reach to the electrode. At second step, lithium ions are desolvated just before lithium insertion in Si, and forms Li_xSi alloys at third step. At this step just after forming Li_xSi alloys, electrolyte solutions should react with Li_xSi.

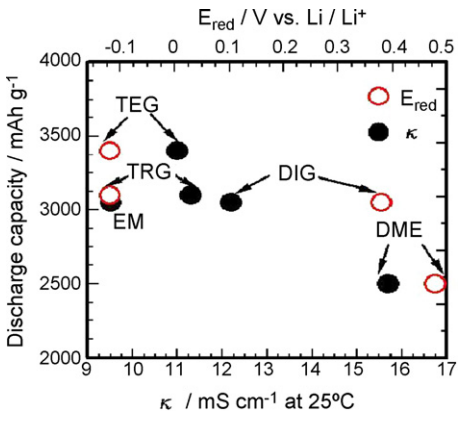

Fig. 10. Relationships among a discharge capacity of Li/Si + C cell at first cycle, a reduction potential (E_{red}) of *n*-glymes and an electrolyte conductivity (κ) of EM/*n*-glymes, I_{ps} = 0.5 mA cm^{-2}, charge–discharge cut-off voltages: 0 and 1.5 V.

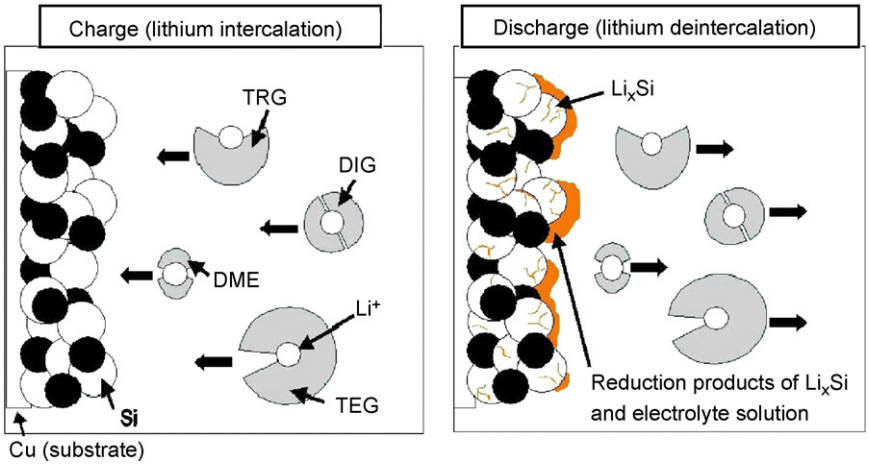

Fig. 11. Proposed mechanism for change in lithium cycling efficiency in Si + C electrodes with EM/*n*-glyme electrolytes.

This irreversible reduction consumes the lithium in the Li_xSi. This consumption of lithium helps the degradation of discharge capacity as well as physical electrode breakdown of Li_xSi. So, discharge capacity depends on the tolerance of *n*-glymes toward reduction (E_{red}), not on the electrolyte conductivity (κ) as shown in Figs. 9 and 10. E_{red} of glymes was high in the order of DME > DIG > EM > TRG > TEG.

3.3. Charge–discharge cycling properties of lithium in Si–C + C electrodes with EM/n-glyme electrolyte solutions

Using Li/Si–C + C coin cells with EM/n-glymes carried out charge–discharge cycling tests of lithium. Figs. 12 and 13 show charge–discharge cycling test results. Fig. 12 shows the relationship among a discharge capacity, a charge–discharge cycling efficiency (E_{ff}) and a cycle number. Fig. 13 shows the relationship among a discharge capacity at first cycle, an electrolyte conductivity (κ) and a reduction potential (E_{red}) of *n*-glymes. Following six results were obtained from these two figures. (1) Discharge capacities depended on the kind of electrolyte solutions. (2) Discharge capacity was high in the order of EM/DIG > EM/TRG ~ EM/TEG > EM > EM/DME. By mixing *n*-glymes to EM, the discharge capacity tended to become larger than that with EM alone, except for DME. (3) There was no distinguishing relation between discharge capacity and E_{red}. (4) With an increase in *k*, the discharge capacity tended to increase except for DME. (5) Cycling stability (E_{ff} versus cycle number) life of all the Li/Si–C + C cells was similar with different electrolytes. (6) Cycling stability of Li/Si–C + C cells was better than those of Si + C cells.

Summarizing these results, primary cause for the better cycle life of Li/Si–C + C cells than Si + C cells is suggested to be the Si–C structure suppressing a physical break-down of Si + C electrode. Additional effect is an influence of the electrolyte solutions. The model of the influence of electrolyte solutions on charge–discharge of lithium in Si–C + C was proposed (Fig. 14). In case of Si–C, Si in dispersed in amorphous SiO_2 and the surface of Si–C material is covered with thin carbon layer. This carbon layer and SiO_2-amorphous of Si–C suppress the large volume change of electrode during charge–discharge [14–16]. Also, this carbon layer may work as an SEI. That is, the SEI, suppresses the reaction between lithium and electrolyte solutions as in case of carbon anodes [17]. So, the discharge capacity did not depend on the tolerance

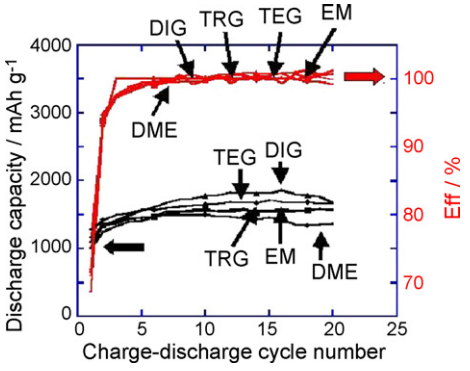

Fig. 12. Relationships among a discharge capacity, a charge–discharge cycling efficiency and a cycle number of Li/Si–C + C cells with EM/glyme electrolytes, I_{ps} = 0.5 mA cm^{-2}, charge–discharge cut-off voltages: 0 and 1.5 V.

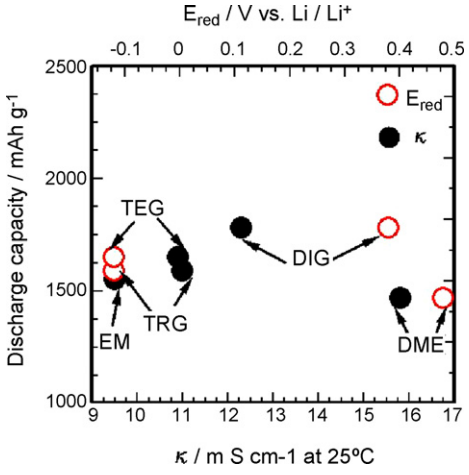

Fig. 13. Relationships among a discharge capacity of Li/Si–C + C cell at first cycle, a reduction potential (E_{red}) of *n*-glymes and an electrolyte conductivity (κ) of EM/*n*-glymes, I_{ps} = 0.5 mA cm^{-2}, charge–discharge cut-off voltages: 0 and 1.5 V.

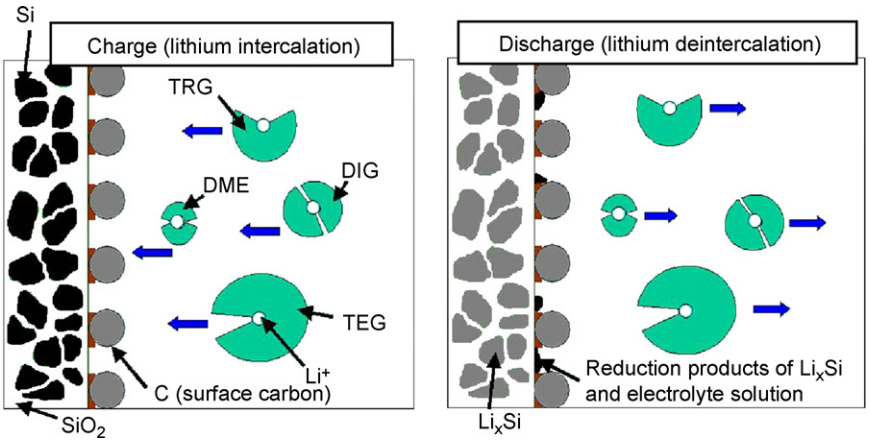

Fig. 14. Proposed mechanism for change in lithium cycling efficiency in Si–C + C electrodes with EM/*n*-glyme electrolytes.

of *n*-glymes toward reduction (E_{red}). Other while, the high conductive electrolyte solutions lead the improvement of homogeneous electrode utilization during dynamic charge–discharge cycling by helping smooth lithium ion migration. So, discharge capacity of Li/Si–C + C cells depends on electrolyte conductivity (κ). κ of EM/glymes was high in the order of EM/DME > EM/DIG > EM/TRG > EM/TEG > EM.

EM/DME exhibited the highest conductivity among electrolytes examined here. However, the discharge capacity of Li/Si–C + C cell was smaller than those of the cells with other glyme based electrolytes. This capacity degradation of Si–C with DME electrolyte is explained as follows. DME has the smallest volume among the solvents examined here. Therefore, DME may pass through the pore of the carbon thin layer and react with lithium in Li_xSi.

4. Conclusion

Influence of electrolyte solutions on charge–discharge properties of Si-based anodes was examined. In case of Li/Si + C cells, by mixing glymes to EM, the discharge capacity tended to become larger than that with EM alone. The cycle life of Li/Si + C cells were approximately the same when different electrolyte solutions were used. Primary reason for the degradation of charge–discharge cycling life is a physical breakdown of Si electrode, being due to the large volume change of electrode by expansion and shrinking of Si by charge and discharge of Li in Si. Also, reactivity of electrolyte solutions toward lithium affects the degradation of charge–discharge capacity. Discharge capacity depended on a reduction potential of glymes, not on an electrolyte conductivity. In case of Li/Si–C + C cells, by mixing *n*-glymes to EM, the discharge capacity tended to become larger than that with EM alone. Cycling life of Li/Si–C + C cells improved, compared with that of Li/Si + C cells. This is due to a suppression of physical breakdown by Si–C structure. Influence of reactivity of electrolyte solutions toward lithium on the degradation of charge–discharge capacity of Li/Si–C + C cells is much smaller than that of Li/Si + C cells. Discharge capacity of Li/Si–C + C cells depended on an electrolyte conductivity, not on a tolerance of *n*-glymes toward reduction The influence of electrolyte solution on charge–discharge cycling behavior of lithium in Si + C and Si–C + C electrodes tended to be rather similar to lithium metal and carbon anodes, respectively.

References

[1] R.A. Huggins, J. Power Sources 81–82 (1999) 13.
[2] N. Tamura, R. Ohshita, M. Fujimoto, M. Kamino, S. Fujitani, J. Electrochem. Soc. 150 (2003) A679.
[3] O. Mao, R.A. Dunlap, J.R. Dahn, J. Electrochem. Soc. 146 (1999) 405.
[4] O. Mao, J.R. Dahn, J. Electrochem. Soc. 146 (1999) 414.
[5] O. Mao, J.R. Dahn, J. Electrochem. Soc. 146 (1999) 423.
[6] L.Y. Beaulien, D. Larcher, R.A. Dunlap, J.R. Dahn, J. Electrochem. Soc. 147 (2000) 3206.
[7] L.Y. Beaulien, K.C. Hewitt, R.L. Turner, A. Bonakdarpur, A.A. Abdo, L. Christensen, K.W. Eberman, L.J. Krause, J.R. Dahn, J. Electrochem. Soc. 150 (2003) A149.
[8] M. Yoshio, H. Wang, K. Fukuda, T. Umeno, N. Dimov, Z. Ogumi, J. Electrochem. Soc. 149 (2002) A1598.
[9] M. Yoshio, S. Kugino, N. Dimov, J. Power Sources 153 (2006) 375.
[10] N. Dimov, S. Kugino, M. Yoshio, Electrochim. Acta 48 (2003) 1579.
[11] X. Yang, J. McBreen, W. Yoon, M. Yoshio, H. Wang, K. Fukuda, T. Umeno, Electrochem. Commun. 4 (2002) 893.
[12] S. Ohara, J. Susuki, K. Sekine, T. Takamura, Electrochemistry 71 (2003) 1126.
[13] T. Takamura, S. Ohara, M. Uehara, J. Susuki, K. Sekine, J. Power Sources 129 (2004) 96.
[14] M. Miyachi, H. Yamamoto, H. Kawai, T. Ohta, M. Shirakawa, Extended Abstracts of 206th Electrochemical Society Meeting, Abs. No. 311, 2004.
[15] T. Morita, N. Takami, Extended Abstracts of 206th Electrochemical Society Meeting, Abs. No. 312, 2004.
[16] Japan Kokai Tokkyo Koho, Japan Patent application JP2004-47404A (2004).
[17] J.O. Besenhard (Ed.), Handbook of Battery Materials, Wiley–VCH, New York, 1999.
[18] D. Aubach, E. Granot, Electrochim. Acta 42 (1997) 697.
[19] S. Tobishima, H. Morimoto, M. Aoki, Y. Saito, T. Inose, T. Fukumoto, T. Kuryu, Electrochim. Acta 49 (2004) 979.